

# Generalized nuclear contacts and momentum distributions

Ronen Weiss, Betzalel Bazak, and Nir Barnea\*

*The Racah Institute of Physics, The Hebrew University, Jerusalem 9190401, Israel*

(Received 7 April 2015; published 17 November 2015)

The general nuclear contact matrices are defined, taking into consideration all partial waves and finite-range interactions, extending Tan's work on the zero range model. The properties of these matrices are discussed and the relations between the contacts and the one-nucleon and two-nucleon momentum distributions are derived. Using these relations, a new asymptotic connection between the one-nucleon and two-nucleon momentum distributions, describing the two-body short-range correlations in nuclei, is obtained. Using available numerical data, we extract a few connections between the different contacts and verify their relations to the momentum distributions. The numerical data also allows us to identify the main nucleon momentum range affected by two-body short-range correlations. Utilizing these relations and the numerical data, we also verify a previous independent prediction-connecting between the Levinger constant and the contacts. This work provides an important indication for the relevance of the contact formalism to nuclear systems, and should open the path for revealing more useful relations between the contacts and interesting quantities of nuclei and nuclear matter.

DOI: [10.1103/PhysRevC.92.054311](https://doi.org/10.1103/PhysRevC.92.054311)

PACS number(s): 25.60.Gc, 05.30.Fk, 67.85.-d

## I. INTRODUCTION

Recently, a new variable, called *the contact*, was defined by Tan [1,2] for a two component Fermi gas interacting via short-range forces. The contact measures the probability to find two unlike fermions close to each other. In a series of theorems, called Tan's relations, many other properties of the system, such as its energy, pressure, and momentum distribution, were connected to the contact. Tan assumes that the range of the interaction is much smaller than the scattering length and the averaged distance between the fermions. Following these theoretical predictions, several experiments were conducted, verifying Tan's relations in ultracold atomic systems consisting of  $^{40}\text{K}$  [3,4] and  $^6\text{Li}$  [5–7] atoms.

Nuclear systems differ from these ultracold atomic systems in many aspects. First, the nucleons are not two-component fermions. Second, while in the atomic systems the strength of the interaction between the atoms and the density can be changed easily, such that Tan's assumptions are satisfied, in nuclear physics it cannot be done. In nuclear systems, the *s*-wave spin-singlet and spin-triplet scattering lengths are about  $-20$  fm and  $5.38$  fm, respectively, and the average distance between two adjacent nucleons is about  $2.4$  fm. The interaction range of the long-range part of the nuclear potential, which is governed by the pion exchange Yukawa force, is about  $\mu^{-1} = \hbar/m_\pi c \approx 1.4$  fm. Thus, in nuclear physics the interaction range is only slightly smaller than the average distance between two particles and the scattering length.

Considering a two-component Fermi gas that obeys Tan's assumptions, the high momentum tail of the momentum distribution  $n(k)$  is connected to the contact  $C$  through the relation  $n(k) \rightarrow C/k^4$  as  $k \rightarrow \infty$ . In nuclear physics, the high-momentum part of the nucleon's momentum distribution is one of the main tools for studying short-range correlations (SRCs) between nucleons (see [8], and references therein). The main

focus in current studies of two-body SRCs (see, e.g., [9–13]) is around the momentum range  $1.5 \text{ fm}^{-1} < k < 3 \text{ fm}^{-1}$ . In a few of these studies it is claimed that higher momentum is affected also by three-body correlations [14]. In this momentum range, a dominance of neutron-proton (*np*) correlated pairs was observed in electron scattering experiments [11]. This *np* dominance is usually explained by the contribution of the tensor force, which affects only spin-triplet *np* pairs. Another observation is that the correlated pairs usually have high relative momentum and low center of mass momentum, i.e., they move approximately back-to-back. Generalizing Tan's relation between the high momentum tail and the contact to nuclear systems should help in understanding more properties of SRCs in nuclei.

In a previous paper [15], we have suggested that it might be fruitful to use the contact formalism in nuclear systems. There we have defined the neutron-proton *s*-wave nuclear contacts and evaluated their average value relating them to the Levinger photoabsorption constant [16]. In this work we generalize the definition of the nuclear contacts from *s*-wave to all partial waves. We also consider finite-range interactions instead of zero range. The result is matrices of nuclear contacts. We discuss the properties of these matrices, and use our generalized contact formalism to relate the nuclear contacts to the one-nucleon and two-nucleon momentum distributions. Doing so, we find an asymptotic relation between these two distributions which is relevant to the study of SRCs in nuclei. This relation is verified by available numerical data. Further analysis of the numerical data and its implications to the contact formalism are also presented.

In this paper we focus on the two-body contacts and on two-body correlations, postponing the discussion of three-body effects to future publications.

## II. THE MATRICES OF NUCLEAR CONTACTS

Consider a two-component Fermi gas that obeys Tan's assumptions. In such a gas, when a spin-up particle *i* gets

\* nir@phys.huji.ac.il

close to a spin-down particle  $j$ , the many-body wave function can be factorized into a product of an asymptotic pair wave function  $\varphi(\mathbf{r}_{ij})$ ,  $\mathbf{r}_{ij} = \mathbf{r}_i - \mathbf{r}_j$ , and a function  $A$ , also called the regular part of  $\Psi$ , describing the residual  $A - 2$  particle system and the pair's center of mass  $\mathbf{R}_{ij} = (\mathbf{r}_i + \mathbf{r}_j)/2$  motion [1,17],

$$\Psi \xrightarrow{r_{ij} \rightarrow 0} \varphi(\mathbf{r}_{ij})A(\mathbf{R}_{ij}, \{\mathbf{r}_k\}_{k \neq i,j}). \quad (1)$$

Due to the suppression of higher partial waves in these systems, the asymptotic pair wave function will be predominantly an  $s$  wave. In particular, in the zero-range model [18] the pair wave function is given by  $\varphi = (1/r_{ij} - 1/a)$ , where  $a$  is the scattering length.

The contact  $C$  is then defined by [1,17]

$$C = 16\pi^2 N_{\uparrow\downarrow} \langle A|A \rangle, \quad (2)$$

where

$$\begin{aligned} \langle A|A \rangle &= \int \prod_{k \neq i,j} d\mathbf{r}_k d\mathbf{R}_{ij} \\ &\times A^\dagger(\mathbf{R}_{ij}, \{\mathbf{r}_k\}_{k \neq i,j}) \cdot A(\mathbf{R}_{ij}, \{\mathbf{r}_k\}_{k \neq i,j}) \end{aligned} \quad (3)$$

and  $N_{\uparrow\downarrow}$  is the number of possible spin-up–spin-down pairs.

In nuclear physics, we have four-component fermions, which are the protons and neutrons with their spin being either up or down. Moreover, the assumption of a zero-range  $s$ -wave interaction is not accurate for nuclei. As a result, few changes must be made in order to generalize the contact formalism to study nuclear systems.

When nucleon  $i$  gets close to nucleon  $j$ , we must abandon the factorization ansatz and write the wave function as a sum of products of two-body  $\varphi_{ij}$  and  $A - 2$ -body  $A_{ij}$  terms. The asymptotic form of the wave function is then given by

$$\Psi \xrightarrow{r_{ij} \rightarrow 0} \sum_{\alpha} \varphi_{ij}^{\alpha}(\mathbf{r}_{ij}) A_{ij}^{\alpha}(\mathbf{R}_{ij}, \{\mathbf{r}_k\}_{k \neq i,j}). \quad (4)$$

Here the index  $ij$  corresponds to one of the three particle pairs: proton-proton ( $pp$ ), neutron-neutron ( $nn$ ), or neutron-proton ( $np$ ). We note that due to symmetry the asymptotic functions are invariant under same-particle permutations. The pair wave functions depend on the total spin of the pair  $s_2$ , and its angular momentum quantum number  $\ell_2$  (with respect to the relative coordinate  $\mathbf{r}_{ij}$ ) which are coupled to create the total pair angular momentum  $j_2$  and projection  $m_2$ . The quantum numbers  $(s_2, \ell_2, j_2, m_2)$  define the pair's channel. In general, the expansion (4) may contain more than one term per channel, however in the limit  $r_{ij} \rightarrow 0$  only the leading term survives. In short, the sum over  $\alpha$  denotes a sum over the four channel quantum numbers  $(s_2, \ell_2, j_2, m_2)$ .

To ensure an  $A$ -body wave function with total angular momentum  $J$  and projection  $M$  the regular functions  $A_{ij}^{\alpha}$  are given by

$$A_{ij}^{\alpha} = \sum_{J_{A-2}, M_{A-2}} \langle j_2 m_2 J_{A-2} M_{A-2} | J M \rangle A_{ij}^{\{s_2, \ell_2, j_2\} J_{A-2}, M_{A-2}}, \quad (5)$$

where  $J_{A-2}$  and  $M_{A-2}$  are the angular momentum quantum numbers with respect to the sum  $\mathbf{J}_{A-2} + \mathbf{L}_{2,CM}$  of the total angular momentum of the residual  $(A - 2)$  particles  $\mathbf{J}_{A-2}$ , and

the orbital angular momentum  $\mathbf{L}_{2,CM}$  corresponding to  $\mathbf{R}_{ij}$ .  $A_{ij}^{\{s_2, \ell_2, j_2\} J_{A-2}, M_{A-2}}$  is a set of functions with angular momentum quantum numbers  $J_{A-2}$  and  $M_{A-2}$ , which depends also on the numbers  $s_2, \ell_2, j_2$ . The pair wave function is given by

$$\varphi_{ij}^{\alpha} \equiv \varphi_{ij}^{(\ell_2 s_2) j_2 m_2} = [\varphi_{ij}^{\{s_2, j_2\} \ell_2} \otimes \chi_{s_2}]^{j_2 m_2}, \quad (6)$$

where  $\chi_{s_2 \mu_s}$  is the two-body spin function, and  $\varphi_{ij}^{\{s_2, j_2\} \ell_2 \mu_{\ell}}(\mathbf{r}_{ij}) = \varphi_{ij}^{\{\ell_2, s_2, j_2\}}(\mathbf{r}_{ij}) Y_{\ell_2 \mu_{\ell}}(\hat{\mathbf{r}}_{ij})$ . For clarity, when angular momentum indices are written without any brackets they denote the relevant angular momentum quantum numbers of the function. When the indices are in curly brackets, it means that the function depends on these numbers but they do not denote the angular momentum of the function. When two indices are inside round brackets, it means that the angular momentum of the function is created by a coupling of these two indices.

An important property of the set of asymptotic functions  $\{\varphi_{ij}^{\alpha}\}$  is that they are “universal”, in the limited sense that they do not depend on a specific nucleus or on a specific nuclear state. This is a reasonable assumption, because when two particles are close together they interact with each other and the background of the  $A - 2$  particle system can be ignored. This point was proved by Amado [19,20] for a large class of Hamiltonians that include only local two-body forces. Under these assumptions the asymptotic expansion, Eq. (4), contains only one term per channel, and the functions  $\{\varphi_{ij}^{\alpha}\}$  depend only on the details of the nuclear two-body potentials. Thus, they are independent of the specific nuclear state. Amado's arguments can be easily generalized to include also three-body and/or nonlocal forces. In these cases it can be shown that the asymptotic pair functions  $\{\varphi_{ij}^{\alpha}\}$  depend only on the potential and not on the nucleus or the nuclear state. Again, in general there may be more than one function per channel but in the limit  $r_{ij} \rightarrow 0$  these functions collapse into a single leading term.

Since the  $A_{ij}^{\alpha}$  functions are not generally orthogonal for different  $\alpha$ , we are led to define matrices of nuclear contacts in the following way:

$$C_{ij}^{\alpha\beta}(JM) = 16\pi^2 N_{ij} \langle A_{ij}^{\alpha} | A_{ij}^{\beta} \rangle. \quad (7)$$

As before,  $ij$  stands for one of the pairs:  $pp$ ,  $nn$ , or  $np$ ,  $N_{ij}$  is the number of  $ij$  pairs, and  $\alpha$  and  $\beta$  are the matrix indices. We also denote  $\alpha = (s_{\alpha}, \ell_{\alpha}, j_{\alpha}, m_{\alpha})$  and  $\beta = (s_{\beta}, \ell_{\beta}, j_{\beta}, m_{\beta})$ . One can see that if  $m_{\alpha} \neq m_{\beta}$ , then  $C_{ij}^{\alpha\beta}(JM) = 0$ , but it is not generally true for  $j_2, s_2$ , or  $\ell_2$ . For spherical nuclei ( $J = 0$ ) we do get  $C_{ij}^{\alpha\beta}(JM) = 0$  if  $j_{\alpha} \neq j_{\beta}$ . For  $pp$  and  $nn$  pairs, Pauli's exclusion principle tells us that unless  $s_{\alpha} + \ell_{\alpha}$  is even, we have  $A_{pp}^{\alpha} = A_{nn}^{\alpha} = 0$ , so  $C_{pp}^{\alpha\beta} = C_{nn}^{\alpha\beta} = 0$  if  $s_{\alpha} + \ell_{\alpha}$  or  $s_{\beta} + \ell_{\beta}$  are odd. Moreover, if  $\Psi$  is the ground state of the nucleus, or any eigenstate of the nuclear Hamiltonian, then  $\Psi$  has a well defined parity.  $\varphi_{ij}^{\alpha}$  has a parity of  $(-1)^{\ell_{\alpha}}$ , so it dictates the parity of  $A_{ij}^{\alpha}$ . Thus,  $C_{ij}^{\alpha\beta}(JM) = 0$  for  $\alpha$  and  $\beta$  such that  $\ell_{\alpha}$  and  $\ell_{\beta}$  have different parities.

Since the projection  $M$  is usually unknown in experiments, it is useful to define the averaged nuclear contacts:

$$C_{ij}^{\alpha\beta} = \frac{1}{2J+1} \sum_M C_{ij}^{\alpha\beta}(JM). \quad (8)$$

According to this definition, we have three matrices of averaged contacts, one for each kind of nucleon-nucleon pair. We note that the averaged contacts still depend on  $J$ , but we will not write it explicitly. Using Clebsch-Gordan identities one can prove that if  $m_\alpha \neq m_\beta$  or  $j_\alpha \neq j_\beta$ , then  $C_{ij}^{\alpha\beta} = 0$ , and also that the averaged contacts are independent of  $m_\alpha$  and  $m_\beta$ . The averaged contacts inherit the properties of the nonaveraged contacts  $C_{ij}^{\alpha\beta}(JM)$  regarding parity and Pauli's principle.

Concluding, for a given  $\alpha$ , the relevant  $\beta$ 's such that  $C_{ij}^{\alpha\beta}$  can be different from zero must obey  $j_\beta = j_\alpha$  and  $m_\beta = m_\alpha$ . Since,  $s_2 = 0, 1$  there are four  $(s_2, \ell_2)$  pairs that can create a given  $j_\alpha \neq 0$ :  $(0, j_\alpha)$ ,  $(1, j_\alpha)$ ,  $(1, j_\alpha - 1)$ , and  $(1, j_\alpha + 1)$ . The first two options have the same parity of  $\ell_2$  and the last two have the opposite parity. For  $j_\alpha = 0$  we have only two possible  $(s_2, \ell_2)$  pairs:  $(0, 0)$  and  $(1, 1)$ , which have different parity of  $\ell_2$ . Thus, in general the matrices  $C_{ij}^{\alpha\beta}$  are built from  $2 \times 2$  blocks, except for the two  $1 \times 1$  blocks associated with the  $j_2 = 0$  case. Each block has a well-defined  $j_2, m_2$  values. For any  $j_2 \neq 0$  there are two blocks, one with  $(s_2, \ell_2) = (0, j_2), (1, j_2)$  and the other with  $(s_2, \ell_2) = (1, j_2 - 1), (1, j_2 + 1)$ . For  $pp$  and  $nn$  pairs, Pauli's principle dictates that any matrix element with an odd  $s_2 + \ell_2$  is zero, so some of the  $2 \times 2$  blocks are reduced into two  $1 \times 1$  blocks.

In a previous paper [15] we have defined the  $s$ -wave nuclear contacts,  $C_{ij}^{s_2}(JM)$ , for  $s_2 = 0, 1$ . The definition there was slightly different from the current one, as the two-body spin functions were included into the regular  $(A - 2)$  particle function  $A_{ij}^\alpha$ . In our current definition, we have four diagonal  $s$ -wave contacts  $C_{ij}^{\alpha_0\alpha_0}$  and  $C_{ij}^{\alpha_1\mu\alpha_1\mu}$ , where  $\alpha_0 = (s_2 = 0, \ell_2 = 0, j_2 = 0, m_2 = 0)$ ,  $\alpha_1\mu = (s_2 = 1, \ell_2 = 0, j_2 = 1, m_2 = \mu)$ , and  $\mu = -1, 0, 1$ . The relations between the two definitions are

$$C_{ij}^{s_2=0}(JM) = C_{ij}^{\alpha_0\alpha_0}(JM), \quad (9)$$

$$C_{ij}^{s_2=1}(JM) = \sum_{\mu=-1}^1 C_{ij}^{\alpha_1\mu\alpha_1\mu}(JM). \quad (10)$$

Averaging over  $M$  and using the fact that the averaged contacts are independent of  $m_2$  we get

$$C_{ij}^{s_2=0} = C_{ij}^{\alpha_0\alpha_0}, \quad (11)$$

$$C_{ij}^{s_2=1} = \sum_{\mu=-1}^1 C_{ij}^{\alpha_1\mu\alpha_1\mu} = 3C_{ij}^{\alpha_1\mu\alpha_1\mu}. \quad (12)$$

We also note that the previously defined  $s$ -wave contacts,  $C_{ij}^{s_2}(JM)$ , are actually independent of  $M$ . Thus, also  $C_{ij}^{\alpha_0\alpha_0}(JM)$  and  $\sum_{\mu=-1}^1 C_{ij}^{\alpha_1\mu\alpha_1\mu}(JM)$  are independent of  $M$ .

It should be mentioned that the factorization of the wave function given in Eq. (4) was used before in the study of nuclear SRCs, see, e.g., [8] and references therein. In these works the relation between the asymptotic many-body wave function and the deuteron wave function was utilized, and the corresponding contact was defined, see, e.g., [21] Eq. (29). However, it was assumed that the nuclear contact is a single number and the general structure of nuclear contact matrix was not defined or analyzed. In the following we will demonstrate the utility of the

general contact formalism, deriving analytic relations between the nuclear one-body and two-body momentum distributions.

### III. MOMENTUM DISTRIBUTIONS

#### A. The two-nucleon momentum distribution

In the following we will utilize the above generalized contact formalism to find a relation between the two-nucleon momentum distribution and the nuclear contacts.

Let us denote by  $f_{ij}^{JM}(\mathbf{k} + \mathbf{K}/2, -\mathbf{k} + \mathbf{K}/2)$  the density probability to find a pair of nucleons,  $ij \in \{pp, nn, pn\}$ , with any particle of type  $i$  with momentum  $\mathbf{k} + \mathbf{K}/2$  and any particle of type  $j$  with momentum  $-\mathbf{k} + \mathbf{K}/2$ .  $J$  and  $M$  are the angular momentum quantum numbers of the nuclear wave function  $\Psi$ . Working in the momentum space

$$\tilde{\Psi}(\mathbf{k}_1, \dots, \mathbf{k}_A) = \int \prod_{n=1}^A d^3 r_n \Psi e^{i \sum_n \mathbf{k}_n \cdot \mathbf{r}_n}, \quad (13)$$

and we can write

$$\begin{aligned} & f_{ij}^{JM}(\mathbf{k} + \mathbf{K}/2, -\mathbf{k} + \mathbf{K}/2) \\ &= N_{ij} \int \prod_{m \neq i, j} \frac{d^3 k_m}{(2\pi)^3} |\tilde{\Psi}(\mathbf{k}_1, \dots, \mathbf{k}_i = \mathbf{k} + \mathbf{K}/2, \dots, \\ & \quad \mathbf{k}_j = -\mathbf{k} + \mathbf{K}/2, \dots, \mathbf{k}_A)|^2, \end{aligned} \quad (14)$$

where  $A$  is the number of nucleons,  $N_{ij}$  is the number of  $ij$  pairs, and we notice that  $f_{ij}^{JM}$  is normalized in such way that  $\int f_{ij}^{JM} \frac{d^3 k}{(2\pi)^3} \frac{d^3 K}{(2\pi)^3} = N_{ij}$ .

In the limit  $k \rightarrow \infty$  the main contribution to  $f_{ij}^{JM}$  comes from the asymptotic  $\mathbf{r}_{ij} \rightarrow 0$  part of the wave function, given in Eq. (4). All other terms will cancel each other due to the fast oscillating  $\exp(i\mathbf{k} \cdot \mathbf{r}_{ij})$  factor. Substituting  $\tilde{\Psi}$  into Eq. (14), and using Eq. (4) we get

$$\begin{aligned} & f_{ij}^{JM}(\mathbf{k} + \mathbf{K}/2, -\mathbf{k} + \mathbf{K}/2) \\ &= N_{ij} \int \prod_{m \neq i, j} \frac{d^3 k_m}{(2\pi)^3} \\ & \quad \times \left| \int \prod_{n \neq i, j}^A d^3 r_n d^3 r_{ij} d^3 R_{ij} \sum_{\alpha} \varphi_{ij}^{\alpha}(\mathbf{r}_{ij}) A_{ij}^{\alpha} \right. \\ & \quad \left. \times \exp\left(i\mathbf{k} \cdot \mathbf{r}_{ij} + i\mathbf{K} \cdot \mathbf{R}_{ij} + \sum_{n \neq i, j} i\mathbf{k}_n \cdot \mathbf{r}_n\right) \right|^2. \end{aligned} \quad (15)$$

We will define now

$$F_{ij}^{JM}(\mathbf{k}) = \int \frac{d^3 K}{(2\pi)^3} f_{ij}^{JM}(\mathbf{k} + \mathbf{K}/2, -\mathbf{k} + \mathbf{K}/2). \quad (16)$$

$F_{ij}^{JM}$  is the density probability to find an  $ij$  pair with relative momentum  $\mathbf{k}$ , and it obeys the normalization condition  $\int F_{ij}^{JM}(\mathbf{k}) \frac{d^3 k}{(2\pi)^3} = N_{ij}$ . We can now substitute the asymptotic form of  $f_{ij}^{JM}$ , Eq. (15), into the definition of  $F_{ij}^{JM}$ . In the resulting expression we can separate the integration over  $\mathbf{r}_{ij}$

from the rest of the coordinates. Using the notation

$$\tilde{\varphi}_{ij}^\alpha(\mathbf{k}) = \int d^3r \varphi_{ij}^\alpha(\mathbf{r}) \exp(i\mathbf{k} \cdot \mathbf{r}) \quad (17)$$

and

$$\tilde{A}_{ij}^\alpha = \int \prod_{n \neq i, j} d^3r_n d^3R_{ij} A_{ij}^\alpha \exp\left(i\mathbf{K} \cdot \mathbf{R}_{ij} + \sum_{n \neq i, j} i\mathbf{k}_n \cdot \mathbf{r}_n\right), \quad (18)$$

we get

$$F_{ij}^{JM}(\mathbf{k}) = N_{ij} \sum_{\alpha, \beta} \tilde{\varphi}_{ij}^{\alpha\dagger}(\mathbf{k}) \tilde{\varphi}_{ij}^\beta(\mathbf{k}) \int \prod_{m \neq i, j} \frac{d^3k_m}{(2\pi)^3} \frac{d^3K}{(2\pi)^3} \tilde{A}_{ij}^{\alpha\dagger} \tilde{A}_{ij}^\beta. \quad (19)$$

Noting the equality

$$\int \prod_{m \neq i, j} \frac{d^3k_m}{(2\pi)^3} \frac{d^3K}{(2\pi)^3} \tilde{A}_{ij}^{\alpha\dagger} \tilde{A}_{ij}^\beta = \int \prod_{n \neq i, j} d^3r_n d^3R_{ij} A_{ij}^{\alpha\dagger} A_{ij}^\beta, \quad (20)$$

we obtain the following asymptotic  $k \rightarrow \infty$  expression for the two nucleon momentum distribution,

$$F_{ij}^{JM}(\mathbf{k}) = \sum_{\alpha, \beta} \tilde{\varphi}_{ij}^{\alpha\dagger}(\mathbf{k}) \tilde{\varphi}_{ij}^\beta(\mathbf{k}) \frac{C_{ij}^{\alpha\beta}(JM)}{16\pi^2}. \quad (21)$$

Here we have used the definition of the contacts from Eq. (7). Averaging over  $M$ , we get the asymptotic relation

$$F_{ij}(\mathbf{k}) = \sum_{\alpha, \beta} \tilde{\varphi}_{ij}^{\alpha\dagger}(\mathbf{k}) \tilde{\varphi}_{ij}^\beta(\mathbf{k}) \frac{C_{ij}^{\alpha\beta}}{16\pi^2}, \quad (22)$$

where  $F_{ij} = (2J + 1)^{-1} \sum_M F_{ij}^{JM}$ , and  $C_{ij}^{\alpha\beta}$  are the averaged contacts defined in Eq. (8). Like  $C_{ij}^{\alpha\beta}$ , also  $F_{ij}$  depends implicitly on  $J$ .

### B. The one-nucleon momentum distribution

We would like to relate now the nuclear contacts also to the one-nucleon momentum distributions. The following derivation is based on Tan's derivation for the two-body case in atomic systems [1]. We first focus on the proton's momentum distribution  $n_p^{JM}(\mathbf{k})$ . Normalized to the number of protons in the system  $Z$ ,  $\int \frac{d^3k}{(2\pi)^3} n_p^{JM}(\mathbf{k}) = Z$ ,  $n_p^{JM}$  is given by

$$n_p^{JM}(\mathbf{k}) = Z \int \prod_{l \neq p} \frac{d^3k_l}{(2\pi)^3} |\tilde{\Psi}(\mathbf{k}_1, \dots, \mathbf{k}_p = \mathbf{k}, \dots, \mathbf{k}_A)|^2, \quad (23)$$

where  $p$  is any proton.

In the  $k \rightarrow \infty$  limit the main contribution to  $n_p^{JM}$  emerges from the asymptotic parts of the wave function, i.e., from  $r_{ps} = |\mathbf{r}_p - \mathbf{r}_s| \rightarrow 0$ , for any particle  $s \neq p$ , being proton or neutron. In this limit

$$\tilde{\Psi}(\mathbf{k}_1, \dots, \mathbf{k}_p = \mathbf{k}, \dots, \mathbf{k}_A) = \sum_{s \neq p} \sum_{\alpha} \tilde{\varphi}_{ps}^\alpha((\mathbf{k} - \mathbf{k}_s)/2) \times \tilde{A}_{ps}^\alpha(\mathbf{K}_{ps} = \mathbf{k} + \mathbf{k}_s, \{\mathbf{k}_j\}_{j \neq p, s}), \quad (24)$$

where  $\mathbf{K}_{ps}$  is the center of mass momentum of the  $ps$  pair. Substituting  $\mathbf{k}_s = \mathbf{K}_{ps} - \mathbf{k}$  we get

$$\tilde{\Psi} = \sum_{s \neq p} \sum_{\alpha} \tilde{\varphi}_{ps}^\alpha(\mathbf{k} - \mathbf{K}_{ps}/2) \tilde{A}_{ps}^\alpha(\mathbf{K}_{ps}, \{\mathbf{k}_j\}_{j \neq p, s}). \quad (25)$$

We note that  $\mathbf{k}$  is fixed in Eq. (23) while integrating over all other momenta. Therefore we can replace the integration  $\int d\mathbf{k}_s$  with integration over the pair's center of mass momentum  $\int d\mathbf{K}_{ps}$ . Since  $A_{ps}^\alpha$  is regular,  $\tilde{A}_{ps}^\alpha$  will be significant only if  $\mathbf{K}_{ps}$  is not much larger than the nuclear Fermi momentum and therefore much smaller than  $k$ . We can expand  $\tilde{\varphi}_{ps}^\alpha$  around  $\mathbf{k}$ ,

$$\tilde{\varphi}_{ps}^\alpha(\mathbf{k} - \mathbf{K}_{ps}/2) \cong \tilde{\varphi}_{ps}^\alpha(\mathbf{k}) - \frac{\mathbf{K}_{ps}}{2} \cdot \nabla_{\mathbf{k}} \tilde{\varphi}_{ps}^\alpha(\mathbf{k}) + \dots, \quad (26)$$

keep only the leading order, which is a good approximation for any power-law function, and obtain

$$\tilde{\Psi} \cong \sum_{s \neq p} \sum_{\alpha} \tilde{\varphi}_{ps}^\alpha(\mathbf{k}) \tilde{A}_{ps}^\alpha(\mathbf{K}_{ps}, \{\mathbf{k}_j\}_{j \neq p, s}). \quad (27)$$

We can see that  $\tilde{A}_{ps}^\alpha$  still depends explicitly on the center of mass momentum  $\mathbf{K}_{ps}$ .

Substituting this result into Eq. (23), we get summations over particles  $s$  and  $s'$  different from  $p$ . The contribution of nondiagonal  $s \neq s'$  terms, will be significant only for  $\mathbf{k}_s \approx \mathbf{k}_{s'} \approx -\mathbf{k}$ . In this case  $k, k_s, k_{s'} \rightarrow \infty$  together, which is clearly a three-body effect, and we expect it to be less important than the leading two-body contribution [22]. Consequently, we only consider the diagonal elements and obtain

$$n_p^{JM}(\mathbf{k}) = Z \sum_{s \neq p} \sum_{\alpha, \beta} \int \prod_{l \neq p, s} \frac{d^3k_l}{(2\pi)^3} \frac{d^3K_{ps}}{(2\pi)^3} \tilde{\varphi}_{ps}^{\alpha\dagger}(\mathbf{k}) \tilde{\varphi}_{ps}^\beta(\mathbf{k}) \times \tilde{A}_{ps}^{\alpha\dagger}(\mathbf{K}_{ps}, \{\mathbf{k}_j\}_{j \neq p, s}) \tilde{A}_{ps}^\beta(\mathbf{K}_{ps}, \{\mathbf{k}_j\}_{j \neq p, s}). \quad (28)$$

We will now divide the sum  $\sum_{s \neq p}$  into a sum over protons and a sum over neutrons  $\sum_{p' \neq p} + \sum_n$ . Since the asymptotic functions  $A_{pp'}^\alpha$  and  $\varphi_{pp'}^\alpha$  are the same for all  $pp'$  pairs we can take them out of the sum. The same holds for the  $np$  pairs. As a result we get

$$n_p^{JM}(\mathbf{k}) = \sum_{\alpha, \beta} \tilde{\varphi}_{pp}^{\alpha\dagger}(\mathbf{k}) \tilde{\varphi}_{pp}^\beta(\mathbf{k}) Z(Z-1) \langle A_{pp}^\alpha | A_{pp}^\beta \rangle + \sum_{\alpha, \beta} \tilde{\varphi}_{pn}^{\alpha\dagger}(\mathbf{k}) \tilde{\varphi}_{pn}^\beta(\mathbf{k}) N Z \langle A_{pn}^\alpha | A_{pn}^\beta \rangle. \quad (29)$$

Here  $N$  is the number of neutrons in the system. Using the definition of the contacts, Eq. (7), we see that for  $k \rightarrow \infty$

$$n_p^{JM}(\mathbf{k}) = \sum_{\alpha, \beta} \tilde{\varphi}_{pp}^{\alpha\dagger}(\mathbf{k}) \tilde{\varphi}_{pp}^\beta(\mathbf{k}) \frac{2C_{pp}^{\alpha\beta}(JM)}{16\pi^2} + \sum_{\alpha, \beta} \tilde{\varphi}_{pn}^{\alpha\dagger}(\mathbf{k}) \tilde{\varphi}_{pn}^\beta(\mathbf{k}) \frac{C_{pn}^{\alpha\beta}(JM)}{16\pi^2}. \quad (30)$$

Averaging over  $M$  we further obtain the relation between the averaged contacts and the averaged protons' momentum



distribution  $n_p(\mathbf{k}) = (2J + 1)^{-1} \sum_M n_p^{JM}(\mathbf{k})$  for  $k \rightarrow \infty$ :

$$n_p(\mathbf{k}) = \sum_{\alpha,\beta} \tilde{\varphi}_{pp}^{\alpha\ddagger}(\mathbf{k}) \tilde{\varphi}_{pp}^{\beta}(\mathbf{k}) \frac{2C_{pp}^{\alpha\beta}}{16\pi^2} + \sum_{\alpha,\beta} \tilde{\varphi}_{pn}^{\alpha\ddagger}(\mathbf{k}) \tilde{\varphi}_{pn}^{\beta}(\mathbf{k}) \frac{C_{pn}^{\alpha\beta}}{16\pi^2}. \quad (31)$$

We note that  $n_p(\mathbf{k})$  still depends on  $J$ . Similarly, for the neutrons:

$$n_n(\mathbf{k}) = \sum_{\alpha,\beta} \tilde{\varphi}_{nn}^{\alpha\ddagger}(\mathbf{k}) \tilde{\varphi}_{nn}^{\beta}(\mathbf{k}) \frac{2C_{nn}^{\alpha\beta}}{16\pi^2} + \sum_{\alpha,\beta} \tilde{\varphi}_{pn}^{\alpha\ddagger}(\mathbf{k}) \tilde{\varphi}_{pn}^{\beta}(\mathbf{k}) \frac{C_{pn}^{\alpha\beta}}{16\pi^2}. \quad (32)$$

Comparing Eqs. (31) and (32) to Eq. (22), we can see that for  $k \rightarrow \infty$  there is a simple relation between the one-nucleon and the two-nucleon momentum distributions:

$$n_p(\mathbf{k}) = 2F_{pp}(\mathbf{k}) + F_{pn}(\mathbf{k}), \quad (33)$$

$$n_n(\mathbf{k}) = 2F_{nn}(\mathbf{k}) + F_{pn}(\mathbf{k}). \quad (34)$$

These connections seem intuitive if we assume that a nucleon will have high momentum  $\mathbf{k}$  only if there is another nucleon close to it with opposite momentum  $-\mathbf{k}$ . In this case, if we find a proton with high momentum  $\mathbf{k}$  we know that we will find close to it a neutron or a proton, that is a correlated  $pp$  or  $np$  pair with relative momentum  $\mathbf{k}$ . Notice that the factor of 2 before  $F_{pp}$  and  $F_{nn}$  in Eqs. (33), (34), can be also explained in this picture by the fact that for example a  $pp$  pair with momenta  $(-\mathbf{k}, \mathbf{k})$  has a relative momentum  $-\mathbf{k}$  even though there is a proton with momentum  $\mathbf{k}$  in this pair. It means that such a pair will be counted for  $n_p(\mathbf{k})$  but not for  $F_{pp}(\mathbf{k})$  and the factor of 2 takes it into consideration.

These relations emphasize the importance of the two-body correlations to the high momentum one-nucleon distribution. As mentioned before, the picture of short-range correlated pairs of nucleons with back-to-back momentum is one of the main features of SRCs in nuclei, and the above relations between the one-nucleon and two-nucleon momentum distributions give a theoretical support to this picture.

In Ref. [21] some relations between the one-nucleon and the two-nucleon momentum distributions are discussed. There, based only on numerical calculations, it is claimed that the high momentum tail of the one-nucleon momentum distribution is proportional to the deuteron momentum distribution. Moreover, it is similarly claimed that the two-nucleon momentum distribution is also proportional to the deuteron momentum distribution for high momentum. The proportional factors in these two cases are approximated to be equal in Ref. [21] for all the possible pairs:  $pp$ ,  $nn$ , or  $pn$ . It means that in this case the high momentum tails of all these momentum distributions should be equal. Our relations, Eqs. (33) and (34), were derived analytically, and give the correct relations between the different high momentum tails when two-body SRCs are significant and three-body SRCs are negligible. Moreover, there is no reason

to believe that the  $pp$  or  $nn$  high momentum tails will be proportional to the deuteron tail, which consist of a  $pn$  pair. Indeed, this point is demonstrated in the results of Refs. [9] and [23] which show that the relevant  $pp$  and  $nn$  contribution to the momentum distribution are different from the deuteron one. This point is further discussed in the next section, where the numerical data of Ref. [9] is analyzed.

We also note here that similar derivations can be done easily for atomic systems consisting of two-component fermions, denoted by  $\uparrow$  and  $\downarrow$ . The one-body high momentum distribution is already known and given by  $n_{\uparrow}(\mathbf{k}) = n_{\downarrow}(\mathbf{k}) = C/k^4$ . Adjusting the above derivation for the two-nucleon momentum distribution to atomic systems will produce an identical relation between the two-body momentum distribution,  $F_{\uparrow\downarrow}(\mathbf{k})$ , describing the probability to find an  $\uparrow\downarrow$  pair with high relative momentum, and the atomic contact. Explicitly,  $F_{\uparrow\downarrow}(\mathbf{k}) = C/k^4$ . As a result we find that  $n_{\uparrow}(\mathbf{k}) = n_{\downarrow}(\mathbf{k}) = F_{\uparrow\downarrow}(\mathbf{k})$  for high momentum  $\mathbf{k}$ . This relation tells us that also in the ultracold atomic systems the correlated  $\uparrow\downarrow$  pairs have back-to-back momentum, like in nuclear systems.

## IV. ANALYSIS OF NUMERICAL DATA

### A. Momentum distributions

In order to check the validity of our results in actual nuclear systems, we turn now to compare our theoretical predictions to available numerical data. To this end, we will use numerical data of one-nucleon and two-nucleon momentum distributions calculated by Wiringa *et al.* for nuclei with  $A \leq 10$  [9] with the variational Monte Carlo method (VMC), using the realistic Argonne v18 two-nucleon (AV18) [24] and Urbana X three-nucleon (Ubx) [25] potentials. In these VMC results, the calculations of both one-nucleon and two-nucleon momentum distributions were done for nuclei in their ground state. Consequently, the following analysis is limited to the nuclear ground state.

First we check the relation between the one-nucleon and the two-nucleon momentum distributions, Eqs. (33), (34). In Fig. 1 the ratio between  $2F_{pp} + F_{pn}$  and  $n_p$  is presented for various nuclei. We can see that for  $k \rightarrow \infty$  the two quantities coincide and our prediction (33) is indeed satisfied. In Fig. 2 we present the ratio between  $2F_{nn} + F_{pn}$  and  $n_n$ . We show only the results for non-symmetric nuclei, because for symmetric nuclei there is no difference between protons and neutrons in the numerical VMC data. We can see that also here, the ratio  $(2F_{nn} + F_{pn})/n_n \rightarrow 1$  as  $k \rightarrow \infty$  and our prediction (34) is satisfied. This result is obtained for all available nuclei:  ${}^4\text{He}$ ,  ${}^6\text{He}$ ,  ${}^8\text{He}$ ,  ${}^6\text{Li}$ ,  ${}^8\text{Be}$ , and  ${}^{10}\text{B}$ , for both protons and neutrons. For all these nuclei the momentum relations hold for  $4 \text{ fm}^{-1} < k < 5 \text{ fm}^{-1}$ .

The correspondence between our predictions, derived using the contact formalism, and the numerical data is a good indication for the relevance of the contact formalism to nuclear systems. We also learn here that the approximations made in the above theoretical derivations for  $k \rightarrow \infty$  are valid for  $4 \text{ fm}^{-1} < k < 5 \text{ fm}^{-1}$ . This is the first indication for the momentum range which is relevant to the contact formalism in nuclear systems. Moreover, as we mentioned

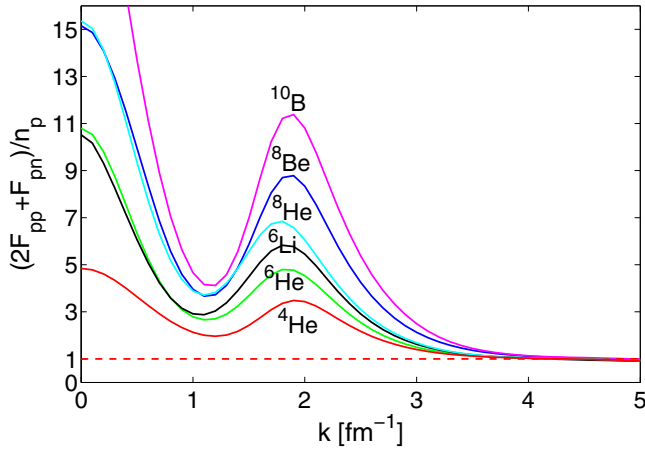


FIG. 1. (Color online) The ratio  $(2F_{pp} + F_{pn})/n_p$  for different nuclei. The numerical data are taken from Ref. [9]. Red line— ${}^4\text{He}$ , green line— ${}^6\text{He}$ , cyan line— ${}^8\text{He}$ , black line— ${}^6\text{Li}$ , blue line— ${}^8\text{Be}$ , and pink line— ${}^{10}\text{B}$ . The dashed red line is the reference  $y = 1$ .

before, in current studies of SRCs in nuclei this momentum range of  $k > 4 \text{ fm}^{-1}$  is believed to be affected by three-body correlations. As explained, Eqs. (33) and (34) are supposed to be satisfied when the two-body correlations are the only significant correlations and every high momentum nucleon has a single nucleon near it with back-to-back momentum. It means that according to this numerical data the momentum range of  $4 \text{ fm}^{-1} < k < 5 \text{ fm}^{-1}$  is affected almost exclusively by two-body SRCs while three-body SRCs are negligible, and that in this momentum range the picture of back-to-back short-range correlated pairs is accurate.

We note that this momentum range of  $4 \text{ fm}^{-1} < k < 5 \text{ fm}^{-1}$  might be model dependent, and it should be verified using other numerical methods, and different nuclear potentials. It should also be mentioned that the VMC method utilizes two and three-body Jastrow correlations in the nuclear wave function.

Hen *et al.* [26] also discuss the possibility that the contact formalism is relevant in nuclear physics. In their work, they

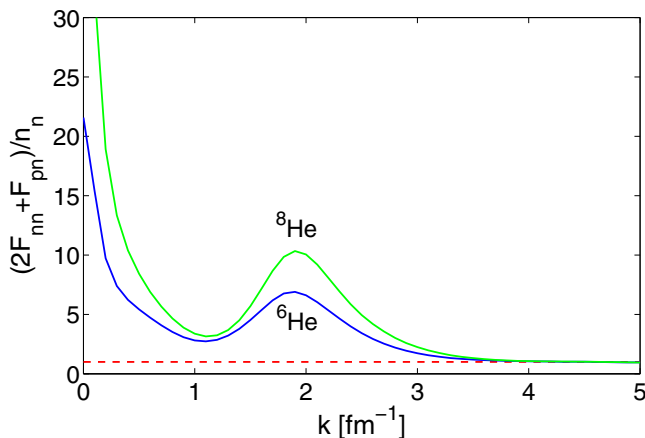


FIG. 2. (Color online) The ratio  $(2F_{nn} + F_{pn})/n_n$  for the non-symmetric nuclei in the numerical data of Ref. [9]. Blue line— ${}^6\text{He}$ , and green line— ${}^8\text{He}$ . The dashed red line is the reference  $y = 1$ .

present an experimental measurement of a  $k^{-4}$  behavior in the proton momentum distribution in the deuteron for  $1.6 \text{ fm}^{-1} < k < 3.2 \text{ fm}^{-1}$ . They also claim that the  $k^{-4}$  behavior exists in heavier nuclei in the same momentum range. As mentioned before, one of the results of the contact formalism in atomic systems is the  $k^{-4}$  tail in the momentum distribution, but this behavior is a direct consequence of the zero-range model. In nuclear systems this model is not accurate, so we can only expect a high momentum tail universal to all nuclei, but not a  $k^{-4}$  behavior. We also note that in the numerical VMC data there is no  $k^{-4}$  tail for nuclei heavier than the deuteron. Moreover, we have found here that the relevant momentum range for the contact formalism in nuclei is  $4 \text{ fm}^{-1} < k < 5 \text{ fm}^{-1}$ , which is higher than the momentum range discussed by Hen *et al.*

### B. The $pp$ and $nn$ contacts along the nuclear chart

We continue now by examining the ratio between  $F_{pp}(\mathbf{k})$  and  $F_{nn}(\mathbf{k})$  in the same nuclei. In the VMC results, this ratio equals 1 for all  $k$  for symmetric nuclei ( $N = Z$ ). Therefore, we are left with the available nonsymmetric nuclei  ${}^6\text{He}$  and  ${}^8\text{He}$ . The relevant results are shown in Fig. 3.

We can see that for  $4 \text{ fm}^{-1} < k < 5 \text{ fm}^{-1}$  the ratio is approximately constant. Inspecting Eq. (22), we see that the only way for this ratio to be constant is that (i) only pairs in  $\alpha, \beta$  states with the same  $k$  dependence of  $\tilde{\varphi}_{ij}^{\alpha\dagger} \tilde{\varphi}_{ij}^{\beta}$  contribute significantly to both  $F_{pp}$  and  $F_{nn}$ , and (ii) both  $pp$  and  $nn$  pairs have the same  $k$  dependence. It is reasonable to assume that the  $s$ -wave contacts are the most significant contacts. For  $pp$  and  $nn$  pairs the only possible nonzero  $s$ -wave contact is  $C_{ij}^{\alpha_0\alpha_0}$ , where  $\alpha_0 \equiv (s_2 = 0, \ell_2 = 0, j_2 = 0, m_2 = 0)$ . This point can be verified numerically through analysis of the angular dependence of the momentum distributions. If the  $s$ -wave contact is indeed dominant we expect to see no angular dependence. If we further assume that  $\tilde{\varphi}_{pp}^{\alpha_0\dagger} \tilde{\varphi}_{pp}^{\alpha_0} = \tilde{\varphi}_{nn}^{\alpha_0\dagger} \tilde{\varphi}_{nn}^{\alpha_0}$ , which seems reasonable from isospin symmetry, then the ratio

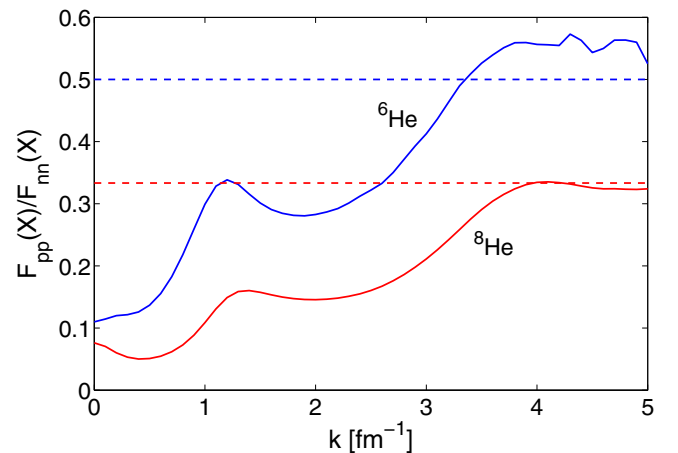


FIG. 3. (Color online) The ratio between  $F_{pp}$  and  $F_{nn}$  in the same nuclei for the available nonsymmetric nuclei in [9]. Blue line— ${}^6\text{He}$ , and red line— ${}^8\text{He}$ . The dashed blue and red lines indicate the value of  $Z/N$  in  ${}^6\text{He}$ , and  ${}^8\text{He}$ , respectively.

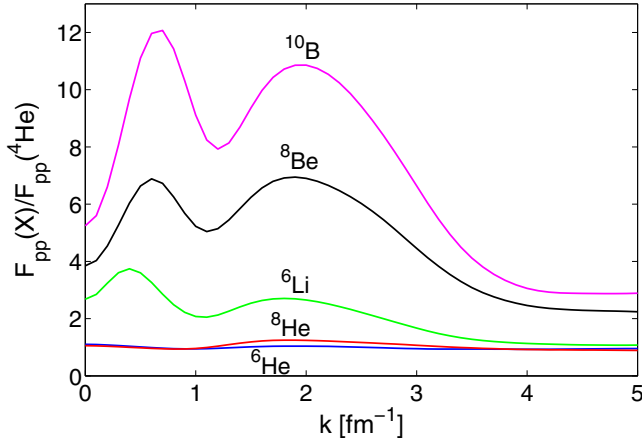


FIG. 4. (Color online) The ratio between  $F_{pp}(X)$  and  $F_{pp}(^4\text{He})$  for the available nuclei  $X$  in the numerical data of Ref. [9]. Blue line— $^6\text{He}$ , red line— $^8\text{He}$ , green line— $^6\text{Li}$ , black line— $^8\text{Be}$ , and pink line— $^{10}\text{B}$ .

between  $F_{pp}$  and  $F_{nn}$  for large momentum equals to the ratio between  $C_{pp}^{\alpha_{00}\alpha_{00}}$  and  $C_{nn}^{\alpha_{00}\alpha_{00}}$ .

We can also see in Fig. 3, that for the two relevant nuclei the ratio  $F_{pp}/F_{nn}$  is close to the ratio  $Z/N$  between the number of protons and neutrons in the nucleus. If this relation turns out to be true in general along the nuclear chart, it means that for a nucleus  $X$  in its ground state, the most significant  $pp$  and  $nn$  contacts are  $C_{pp}^{\alpha_{00}\alpha_{00}}$  and  $C_{nn}^{\alpha_{00}\alpha_{00}}$  and their ratio is given by

$$\frac{C_{pp}^{\alpha_{00}\alpha_{00}}(X)}{C_{nn}^{\alpha_{00}\alpha_{00}}(X)} \approx \frac{Z(X)}{N(X)}, \quad (35)$$

and

$$\varphi_{pp}^{\alpha_{00}\alpha_{00}}(r) = \varphi_{nn}^{\alpha_{00}\alpha_{00}}(r). \quad (36)$$

Here  $Z(X)$  is the number of protons, and  $N(X)$  is the number of neutrons in the nucleus  $X$ . This result is surprising because one might think that the ratio (35) should scale as the ratio between the total number of  $pp$  pairs and the number of  $nn$  pairs in the nucleus, i.e.,  $Z^2/N^2$ . The above result tells us that the number of correlated  $pp$  and  $nn$  pairs in nuclei goes like  $Z$  and  $N$ , respectively. If we check the ratio between  $F_{pp}$  or  $F_{nn}$  and  $F_{pn}$ , no plateau is observed.

We can also examine the ratio between  $F_{pp}$  of nucleus  $X$  and  $F_{pp}$  of another nucleus  $Y$ . The results are presented in Fig. 4, where all the available nuclei are compared to  $^4\text{He}$ .

Here again we see flattening for  $4 \text{ fm}^{-1} < k < 5 \text{ fm}^{-1}$ . This behavior supports the claim that only one contact contributes significantly to  $F_{pp}$ , and so the value of this ratio is just the value of the ratio of this  $pp$  contact in the two different nuclei [see Eq. (22)]. The constant behavior also supports the assumption that the pair wave functions  $\varphi_{pp}^{\alpha\beta}$  are universal along the nuclear chart, because that way the  $k$  dependence indeed vanishes. The average values of this ratio for  $4 \text{ fm}^{-1} \leq k \leq 5 \text{ fm}^{-1}$  are presented in Table I and compared to the ratio between the number of protons in the relevant nuclei and the number of protons in  $^4\text{He}$ . We can see that the two ratios are approximately equal for the different nuclei. If the most significant  $pp$  contact is the  $s$ -wave contact  $C_{pp}^{\alpha_{00}\alpha_{00}}$ , then we

TABLE I. The averaged value of the ratio between  $F_{pp}(X)$  and  $F_{pp}(^4\text{He})$  for  $4 \text{ fm}^{-1} \leq k \leq 5 \text{ fm}^{-1}$  for all the available nuclei in the numerical data of Ref. [9].

$X$	$\langle F_{pp}(X)/F_{pp}(^4\text{He}) \rangle$	$Z(X)/Z(^4\text{He})$
$^6\text{He}$	$0.94 \pm 0.01(1\sigma)$	1
$^8\text{He}$	$0.90 \pm 0.01(1\sigma)$	1
$^6\text{Li}$	$1.09 \pm 0.02(1\sigma)$	1.5
$^8\text{Be}$	$2.31 \pm 0.07(1\sigma)$	2
$^{10}\text{B}$	$2.91 \pm 0.06(1\sigma)$	2.5

can deduce that for nuclei  $X$  and  $Y$  in their ground state:

$$\frac{C_{pp}^{\alpha_{00}\alpha_{00}}(X)}{C_{pp}^{\alpha_{00}\alpha_{00}}(Y)} \approx \frac{Z(X)}{Z(Y)}. \quad (37)$$

For  $F_{nn}$  similar results are observed, therefore we can also deduce that

$$\frac{C_{nn}^{\alpha_{00}\alpha_{00}}(X)}{C_{nn}^{\alpha_{00}\alpha_{00}}(Y)} \approx \frac{N(X)}{N(Y)}. \quad (38)$$

These relations support the claim that the number of correlated  $pp$  and  $nn$  pairs in nuclei is proportional to  $Z$  and  $N$ , respectively.

### C. The $pn$ contacts and the Levinger constant

So far we have studied the properties of the  $pp$  and  $nn$  contacts, now we turn to study the  $pn$  contacts. The  $pn$  contacts might be the most interesting ones because of the dominance of correlated  $pn$  pairs in nuclear SRCs [11]. In order to study the properties of the  $pn$  contacts we examine the variation in  $F_{pn}$  between different nuclei. As in the  $pp$  and  $nn$  cases, also in this case we shall assume that the  $s$  wave is the most dominant partial wave. For a  $pn$  pair in an  $s$  wave there are two possible spin configurations, spin-singlet and spin-triplet. For the deuteron  $^2\text{H}$ , only the spin triplet is relevant as it is a  $J = 1$  state. In Fig. 5 we present the ratio between  $F_{pn}(X)$  and  $n_p(^2\text{H})$  for the available nuclei in the VMC results.

Once again, a constant behavior is seen for  $4 \text{ fm}^{-1} < k < 5 \text{ fm}^{-1}$ . As mentioned before, we have three equal spin triplet  $s$ -wave  $np$  contacts,  $C_{pn}^{\alpha_{1\mu}\alpha_{1\mu}}$ , and one spin-singlet  $s$ -wave  $np$  contact  $C_{pn}^{\alpha_{00}\alpha_{00}}$ . Moreover,  $|\tilde{\varphi}_{pn}^{\alpha_{1\mu}}|^2$  is independent of  $\mu$ . Consequently, we would expect to see a plateau in the ratio  $F_{pn}(X)/n_p(^2\text{H})$ , if either the asymptotic pair wave functions obey the relation  $|\tilde{\varphi}_{pn}^{\alpha_{1\mu}}|^2 = |\tilde{\varphi}_{pn}^{\alpha_{00}}|^2$  or alternatively if the spin-triplet  $s$ -wave contacts are dominant. In the first case we can deduce from the relations between the contacts and the one-nucleon and two-nucleon momentum distributions that asymptotically

$$\begin{aligned} \frac{F_{pn}(X)}{n_p(^2\text{H})} &\approx \frac{3C_{pn}^{\alpha_{10}\alpha_{10}}(X) + C_{pn}^{\alpha_{00}\alpha_{00}}(X)}{3C_{pn}^{\alpha_{10}\alpha_{10}}(^2\text{H})} \\ &= \frac{C_{pn}^{s_2=0}(X) + C_{pn}^{s_2=1}(X)}{C_{pn}^{s_2=1}(^2\text{H})}, \end{aligned} \quad (39)$$

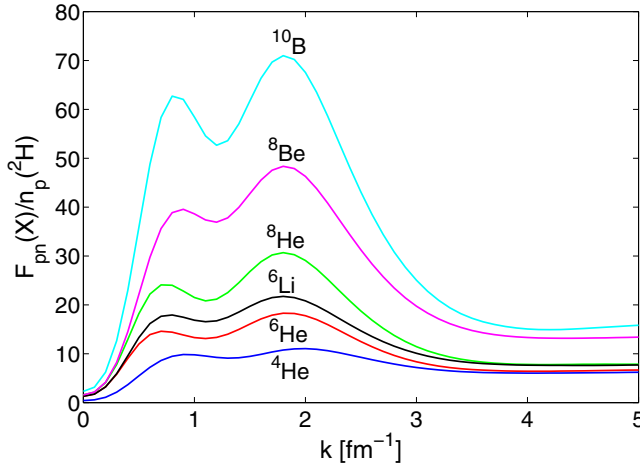


FIG. 5. (Color online) The ratio between  $F_{pn}(X)$  and  $n_p(^2\text{H})$  for the available nuclei  $X$  in the numerical data of Ref. [9]. Blue line— $^4\text{He}$ , red line— $^6\text{He}$ , green line— $^8\text{He}$ , black line— $^6\text{Li}$ , pink line— $^8\text{Be}$ , and cyan line— $^{10}\text{B}$ .

where here we have also used the notation of Eqs. (11) and (12). In the second case we get

$$\frac{F_{pn}(X)}{n_p(^2\text{H})} \approx \frac{C_{pn}^{\alpha_{10}\alpha_{10}}(X)}{C_{pn}^{\alpha_{10}\alpha_{10}}(^2\text{H})} = \frac{C_{pn}^{s_2=1}(X)}{C_{pn}^{s_2=1}(^2\text{H})}. \quad (40)$$

In a previous paper [15], we have predicted that the ratio between the sum of the two  $s$ -wave  $np$  contacts of a nucleus  $X$  in his ground state and the deuteron's  $s$ -wave  $np$  contact is given by

$$\frac{C_{pn}^{s_2=0}(X) + C_{pn}^{s_2=1}(X)}{C_{pn}^{s_2=1}(^2\text{H})} = L \frac{NZ}{A}, \quad (41)$$

where  $L$  is Levinger's constant that relates, at the high energy hand, the photoabsorption cross section of a nucleus to the photoabsorption cross section of the deuteron [16]. Analysis of the experimental results [27] suggest that the  $L$  is approximately a constant along the nuclear chart  $L \approx 5.50 \pm 0.21$  [15]. In [15], we have assumed that the two  $s$ -wave states have the same asymptotic pair wave function in small distances, which corresponds to the first case above. If we were to assume that only the spin-triplet  $np$   $s$  wave is significant, then our result would have been

$$\frac{C_{pn}^{s_2=1}(X)}{C_{pn}^{s_2=1}(^2\text{H})} = L \frac{NZ}{A}. \quad (42)$$

In any of the two cases, we get the relation

$$\frac{F_{pn}(X)}{n_p(^2\text{H})} \approx L \frac{NZ}{A}, \quad (43)$$

that should hold in the high momentum range. For this range of high momentum the ratio between  $F_{pn}$  and  $n_p(^2\text{H})$  is the number of quasideuteron (qd) pairs with high relative momentum in the nucleus. In Table II we present the averaged value of this ratio for  $4 \text{ fm}^{-1} \leq k \leq 5 \text{ fm}^{-1}$  and its multiplication by  $A/NZ$  for each nuclei  $X$ , which should be equal to  $L$  according to the above prediction. One can see that the values

TABLE II. The averaged value of the ratio between  $F_{pn}(X)$  and  $n_p(^2\text{H})$  for  $4 \text{ fm}^{-1} \leq k \leq 5 \text{ fm}^{-1}$  and its multiplication by  $A/NZ$  for all the available nuclei in the numerical VMC results of [9].

$X$	$\langle F_{pn}(X)/n_p(^2\text{H}) \rangle$	$A/NZ \langle F_{pn}(X)/n_p(^2\text{H}) \rangle$
$^4\text{He}$	$6.10 \pm 0.06(1\sigma)$	$6.10 \pm 0.06$
$^6\text{He}$	$6.5 \pm 0.1(1\sigma)$	$4.88 \pm 0.08$
$^8\text{He}$	$7.82 \pm 0.03(1\sigma)$	$5.21 \pm 0.02$
$^6\text{Li}$	$7.63 \pm 0.04(1\sigma)$	$5.09 \pm 0.03$
$^8\text{Be}$	$13.25 \pm 0.08(1\sigma)$	$6.63 \pm 0.04$
$^{10}\text{B}$	$15.3 \pm 0.3(1\sigma)$	$6.1 \pm 0.1$

of the multiplied ratio are close to the above value of  $L$  for all the nuclei and their average value is  $5.7 \pm 0.7(1\sigma)$ . This value is in a very good agreement with the above-mentioned value of  $L$ .

Evaluation of Levinger's constant from the number of qd pairs was done by Benhar *et al.* [28]. In their work, they calculate numerically the number of qd pairs in the nucleus and extract Levinger's constant. In our evaluation we consider only the qd pairs with high relative momentum, which corresponds to small relative distance. Only such qd pairs can be emitted in the photoabsorption process, and therefore only they should be considered.

We have compared here two independent relations between the  $np$  contacts and different properties of nuclei (momentum distribution and photoabsorption cross section) and obtained a good agreement between the two. Doing so, we have also obtained here an established estimation for the leading  $s$ -wave  $np$  contact(s) along the nuclear chart for nuclei in their ground state (in units of the deuteron's  $s$ -wave  $np$  contact).

## V. SUMMARY

Summing up, we have generalized the contact formalism to nuclear systems and defined a matrix of contacts for each particle pair:  $pp$ ,  $nn$ , and  $pn$ . With this generalization we have taken into consideration both different partial waves and finite-range interaction. We have discussed the simple properties of the nuclear contacts and demonstrated the use of the generalized formalism by relating the contacts to the one-nucleon and two-nucleon momentum distributions. As a result we have obtained a relation between these two momentum distributions, which emphasizes the significant contribution of SRCs to the high one-nucleon momentum tail. Using available VMC numerical data [9], calculated with the AV18 and Ubx potentials for nuclei with  $A \leq 10$ , we have verified the above relation and found further relations between the different nuclear contacts. Using few of these new relations and a previous prediction connecting the  $pn$  contacts to the Levinger constant, we have calculated Levinger's constant for the available nuclei and got a good agreement with its experimental value. This is an important indication for the relevance of the contact formalism to nuclear systems, and might open the path to revealing many more interesting relations. We have also learned from the numerical data that the relevant momentum range for the contact's approximations in nuclear systems is  $4 \text{ fm}^{-1} < k < 5 \text{ fm}^{-1}$ . However, we



note that this result might be model dependent. The fact that the relations between the one-nucleon and two-nucleon momentum distribution were satisfied in this momentum range teaches us that for such momenta the two-body SRCs, rather than three-body SRCs, are dominant. Additional numerical or experimental data for both one-nucleon and two-nucleon momentum distributions in more nuclei, also in excited states, including angular-dependence is needed in order to improve

our understanding regarding the properties of the nuclear contacts.

### ACKNOWLEDGMENTS

We would like to thank R. B. Wiringa for his comments and data. This work was supported by the Pazy foundation.

- 
- [1] S. Tan, *Ann. Phys. (NY)* **323**, 2952 (2008); **323**, 2971 (2008); **323**, 2987 (2008).
  - [2] E. Braaten, in *BCS-BEC Crossover and the Unitary Fermi Gas*, edited by W. Zwerger (Springer, Berlin, 2012).
  - [3] J. T. Stewart, J. P. Gaebler, T. E. Drake, and D. S. Jin, *Phys. Rev. Lett.* **104**, 235301 (2010).
  - [4] Y. Sagi, T. E. Drake, R. Paudel, and D. S. Jin, *Phys. Rev. Lett.* **109**, 220402 (2012).
  - [5] G. B. Partridge, K. E. Strecker, R. I. Kamar, M. W. Jack, and R. G. Hulet, *Phys. Rev. Lett.* **95**, 020404 (2005).
  - [6] F. Werner, L. Tarruel, and Y. Castin, *Eur. Phys. J. B* **68**, 401 (2009).
  - [7] E. D. Kuhnle, H. Hu, X.-J. Liu, P. Dyke, M. Mark, P. D. Drummond, P. Hannaford, and C. J. Vale, *Phys. Rev. Lett.* **105**, 070402 (2010).
  - [8] C. Ciofi degli Atti, *Phys. Rep.* **590**, 1 (2015).
  - [9] R. B. Wiringa, R. Schiavilla, S. C. Pieper, and J. Carlson, *Phys. Rev. C* **89**, 024305 (2014).
  - [10] N. Fomin *et al.*, *Phys. Rev. Lett.* **108**, 092502 (2012).
  - [11] O. Hen *et al.* (CLAS Collaboration), *Science* **346**, 614 (2014).
  - [12] M. Alvioli, C. Ciofi degli Atti, and H. Morita, *Phys. Rev. Lett.* **100**, 162503 (2008).
  - [13] J. Arrington, D. Higinbotham, G. Rosner, and M. Sargsian, *Prog. Part. Nucl. Phys.* **67**, 898 (2012).
  - [14] K. Egiyan *et al.* (CLAS Collaboration), *Phys. Rev. Lett.* **96**, 082501 (2006).
  - [15] R. Weiss, B. Bazak, and N. Barnea, *Phys. Rev. Lett.* **114**, 012501 (2015).
  - [16] J. S. Levinger, *Phys. Rev.* **84**, 43 (1951).
  - [17] F. Werner and Y. Castin, *Phys. Rev. A* **86**, 013626 (2012).
  - [18] H. A. Bethe and R. Peierls, *Proc. Roy. Soc.* **148**, 146 (1935).
  - [19] R. D. Amado, *Phys. Rev. C* **14**, 1264 (1976).
  - [20] R. D. Amado and R. M. Woloshyn, *Phys. Lett. B* **62**, 253 (1976).
  - [21] C. Ciofi degli Atti and S. Simula, *Phys. Rev. C* **53**, 1689 (1996).
  - [22] E. Braaten, D. Kang, and L. Platter, *Phys. Rev. Lett.* **106**, 153005 (2011).
  - [23] M. Alvioli, C. Ciofi degli Atti, L. P. Kaptari, C. B. Mezzetti, and H. Morita, *Phys. Rev. C* **87**, 034603 (2013).
  - [24] R. B. Wiringa, V. G. J. Stoks, and R. Schiavilla, *Phys. Rev. C* **51**, 38 (1995).
  - [25] S. C. Pieper, V. R. Pandharipande, R. B. Wiringa, and J. Carlson, *Phys. Rev. C* **64**, 014001 (2001).
  - [26] O. Hen, L. B. Weinstein, E. Piasetzky, G. A. Miller, M. M. Sargsian, and Y. Sagi, *Phys. Rev. C* **92**, 045205 (2015).
  - [27] M. L. Terranova, D. A. De Lima, and J. D. Pinheiro Filho, *Europhys. Lett.* **9**, 523 (1989); O. A. P. Tavares and M. L. Terranova, *J. Phys. G* **18**, 521 (1992).
  - [28] O. Benhar, A. Fabrocini, S. Fantoni, A. Yu. Illarionov, and G. I. Lykasov, *Phys. Rev. C* **67**, 014326 (2003).